Karlsruhe Institute of Technology

Institute of Mechanics

Multiscale modeling of failure in ABS materials

Martin Helbig, Thomas Seelig

15. International Conference on

Deformation, Yield and Fracture of Polymers

Kerkrade, April 2012

Institute of Mechanics
Kaiserstr. 12
D-76131 Karlsruhe
Tel.: +49 (0) 721/ 608-42071
Fax: +49 (0) 721/608-47990
E-Mail: info@ifm.kit.edu
www.ifm.uni-karlsruhe.de

Multiscale modeling of failure in ABS materials

Martin Helbig, Thomas Seelig

Institute of Mechanics, Karlsruhe Institute of Technology (KIT), 76131 Karlsruhe, Germany

Summary: A continuum mechanical description of crazing at different length scales is introduced. The model relies on the idea that distributed crazing contributes to the overall inelastic strain in a direction determined by maximum principal stress. This concept is used in a homogenized model for ABS which explicitely accounts for several microstructural parameters. Numerical simulations are used to investigate material specific aspects in the behaviour of ABS.

Introduction

ABS (acrylonitrile-butadiene-styrene), consists of an amorphous glassy matrix (SAN) and rubber (butadiene) particles. The enhanced fracture toughness and ductility of ABS, compared to neat SAN, relies on microscopic deformation and damage mechanisms, such as void growth, shear yielding and crazing, see e.g. [1],[2],[9]. Despite numerous experimental studies, many details of these micro-mechanisms, their individual contribution to the overall toughness and their dependence on micro-structural parameters (e.g. rubber particle size, void-volume fraction and distribution) are still not well understood. Theoretical models and numerical simulations may provide a deeper understanding of these issues. In the present work a constitutive modeling approach for the effect of crazing at different length scales is suggested and analyzed.

Continuum modeling of crazing

Crazes are localized zones of fibrillated polymer material which form in the direction normal to the maximum principal stress and are able to transfer stress. Under continued loading their growth proceeds until a critical craze thickness, typically of the order of a micron, is reached. Then rupture of the fibrils takes place and the craze turns into a micro-crack. Individual crazes on the level of a homogeneous glassy polymer have been modeled either as discrete cohesive zones, e.g. [7],[10], or using special continuum finite elements as in [8]. In both approaches the craze (or crack) is constrained by the finite element mesh. As an alternative, a constitutive model is presented here which accounts for the essential features of crazing on the continuum level.

Using the additive decomposition of the rate of deformation tensor $\boldsymbol{D} = \boldsymbol{D}^e + \boldsymbol{D}^c$ into an elastic and an inelastic part, a hypoelastic relation for the Jaumann rate of the Cauchy stress can be written as $\overset{\triangledown}{\boldsymbol{\sigma}} = \boldsymbol{E} : (\boldsymbol{D} - \boldsymbol{D}^c)$ where $\boldsymbol{E}$ is the isotropic forth order elasticity tensor. In the present work, crazing is considered as the only source of inelasticity ("craze yielding"). With the direction $\boldsymbol{n}$ of maximum principal stress at the onset of crazing, the inelastic part of the rate of deformation tensor is – similar to [3] – is governed by the flow rule

$$\boldsymbol{D}^c = \dot{\varepsilon}^c \boldsymbol{n} \otimes \boldsymbol{n} \quad , \qquad \dot{\varepsilon}^c = \dot{\varepsilon}_0 \exp\left(\frac{A}{T}\big(\sigma_n - \sigma_c\big)\right) \quad , \qquad \sigma_n = \boldsymbol{n} \cdot \boldsymbol{\sigma} \cdot \boldsymbol{n} \quad . \tag{1}$$

Here, $\dot{\varepsilon}^c$ denotes the equivalent visco-plastic strain rate, A and $\dot{\varepsilon}_0$ are material parameters, and T is the temperature. Crazing is driven by the resolved normal stress on the craze σ_n which has to overcome the craze yield strength $\sigma_c(\varepsilon^c)$. The latter is taken a function of the accumulated inelastic strain, featuring softening upon craze initiation and subsequent rehardening, analogous to the cohesive zone model employed in [7].

Analysis of a single craze

The following example merely serves to illustrate how crazes in the present approach can freely form in arbitrary directions determined by the loading state, independent of the finite element mesh. A single craze which forms at a void in a cubic unit cell therefore is considered. Figure 1 shows half of the unit cell and indicates by the regions in bright grey where crazing has occured under the different types of loading. Figure 1c provides an example of crack formation from a craze zone, modeled by the elimination of finite elements once the local failure criterion of a critical value of inelastic strain is met.

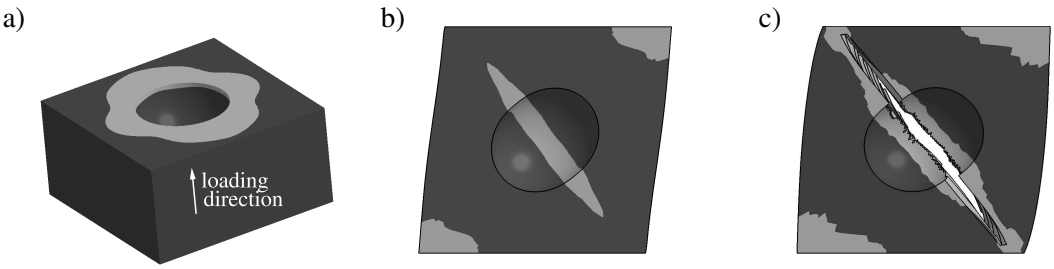

Figure 1: Accumulated inelastic (crazing) strain in a cubic unit cell with a spherical void: a) tension parallel to cell edges, b) and c) different amounts of shear

Homogenized model for distributed crazing in rubber-toughened materials

Experimental studies, e.g. [6], have shown that inelastic deformation of ABS by multiple crazing is accompanied by the formation of many band-like damage zones (as sketched in Fig. 2, left). Similar to individual crazes, yet on a larger length scale and comprising several rubber particles, these zones are oriented normal to the principal loading direction. This suggests that the kinematics of inelastic deformation in (1) is also suitable for the description on the homogenized continuum level of ABS. A constitutive model for ABS that explicitely accounts for the size and volume fraction of rubber particles via appropriate effective properties is set up in the following.

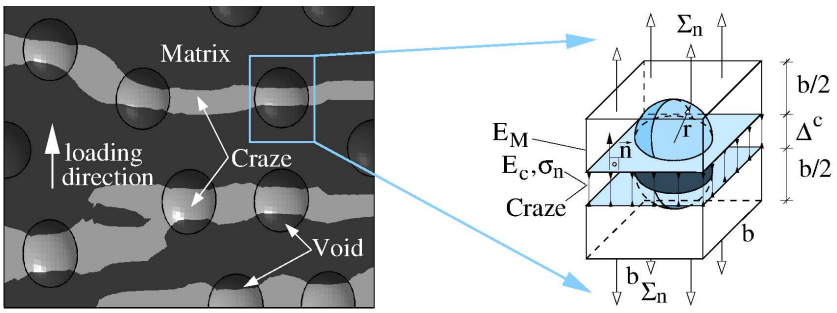

Figure 2: Sketch of localized craze zones in voided polymer matrix (left), single void unit cell with craze zone used for micromechanical modeling (right)

The rubber particles are assumed to cavitate prior to the occurrence of crazing and are considered as voids in the present study. Moreover, despite the oriented nature of the damage zones, the overall elastic behavior of ABS is here for simplicity taken isotropic and represented by effective elastic constants via analytical functions of the porosity. A cubic single void unit cell (Fig. 2, right) is employed to establish proper scaling relations between the inelastic deformation behavior and the microstructure of ABS. Key microstructural parameters, thereby, are the rubber content (porosity) f, the rubber particle size (radius) r, and the maximum craze width Δ^c_{crit} at which local failure takes place. From the porosity $f = \frac{4}{3}\pi r^3/b^3$ and the assumption that at each void a single craze forms (see Fig. 2, right), the average spacing of crazes is

$b(r,f) = r\,(4\pi/3f)^{1/3}$. With the current craze width Δ^c, the overall inelastic strain rate due to distributed crazing is

$$\dot{\varepsilon}^c = \frac{\dot{\Delta}^c}{b+\Delta^c} = \frac{\dot{\Delta}^c}{\Delta^c_{crit}} \left(\frac{r}{\Delta^c_{crit}} \left(\frac{4\pi}{3f}\right)^{1/3} + \frac{\Delta^c}{\Delta^c_{crit}} \right)^{-1} \quad , \tag{2}$$

where for normalization purposes the maximum craze width Δ^c_{crit} is introduced. On the other hand, the driving stress for craze growth (as a function of macroscopic loading $\boldsymbol{\Sigma}$ and porosity) is obtained from unit cell equilibrium considerations as

$$\sigma_n = \boldsymbol{n}\cdot\boldsymbol{\Sigma}\cdot\boldsymbol{n} \left(1 - \pi \left(\frac{3f}{4\pi}\right)^{2/3}\right)^{-1} \quad . \tag{3}$$

The (normalized) craze widening rate $\dot{\Delta}^c/\Delta^c_{crit}$ in (2) is, analogous to (1), governed by an exponential dependence on the driving stress $\sigma_n(f)$ and the craze yield strength $\sigma_c(\Delta^c/\Delta^c_{crit})$. The inelastic part of the rate of deformation tensor on the macroscopic level of homogenized ABS

$$\boldsymbol{D}^c = \dot{\varepsilon}^c\Big(f, r/\Delta^c_{crit}, \Delta^c/\Delta^c_{crit}, \boldsymbol{\Sigma}\Big)\boldsymbol{n}\otimes\boldsymbol{n} \tag{4}$$

hence explicitely depends on the rubber content, the rubber particle size and the amount of crazing. Failure takes place when a critical craze width $\Delta^c = \Delta^c_{crit}$ is reached.

The effect of an increasing amount of distributed crazing on the overall stiffness of ABS is also accounted for in the model. Therefore, the effective elastic constants are (besides their dependence on f) taken to decrease monotonically with increasing Δ^c/b.

Calibration of the macroscopic model

In order to calibrate the material model, uniaxial tensile tests were performed on a commercial ABS material with unknown composition. The rubber content was estimated to $f \approx 0.2$ from the measured elastic stiffness and the known Young's modulus of the SAN matrix. Then the yield strength relation $\sigma_c(\Delta^c/\Delta^c_{crit})$ was fitted so that the overall response of the model for $f \approx 0.2$ agrees with the experimental stress-strain curve (Fig. 3a). Due to the micromechanically based explicit dependence on f, the thus calibrated model captures the influence of the rubber content on the behavior of ABS in a reasonable manner. The predicted decrease of the yield strength and the increase of failure strain with increasing rubber content in Fig. 3a is well known from the literatur, e.g. [4].

The strain rate dependence in the model is calibrated by adjusting the reference strain rate $\dot{\varepsilon}_0$ in (1) to experimental data. The comparison of stress-strain curves over four decades of the strain rate in Fig. 3b shows a good agreement between experimental data and model response.

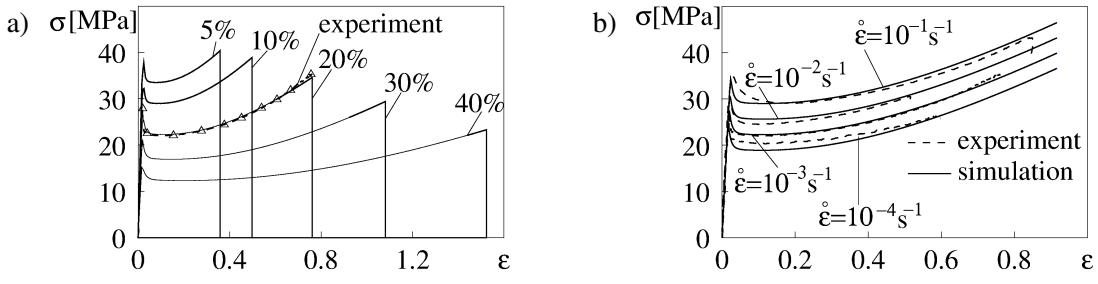

Figure 3: Comparison of experimental true stress vs. log. strain curves with model response: a) effect of rubber content (at $\dot{\varepsilon} = 10^{-3}s^{-1}$), b) effect of strain rate (at $f = 0.2$)

Tensile tests under loading and unloading conditions show a decreasing slope with increasing inelastic deformation, hence a damage evolution takes place (Fig. 4). By adjusting the effective elastic stiffness as a function of craze damage Δ^c/b, this behavior is well described by the model as illustrated in Fig. 4. Not yet captured by the model is the hysteresis in the experiment (dashed line in Fig. 4).

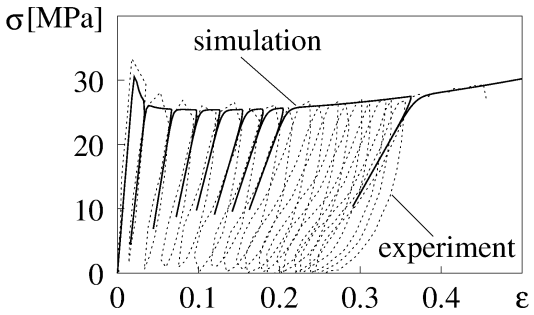

Figure 4: Comparison of experimental true stress vs. log. strain curve and model response for loading and unloading test

Plastic zone in notched specimen

The enhanced fracture toughness of ABS corresponds to the formation of a large stress-whitened ('plastic') zone at a crack tip or notch (Fig. 5a). In a previous study [5], void growth was considered as the dominant damage mechanism in ABS which led to an unrealistic shape of the plastic zone. As an alternative, we here apply the above presented model for distributed crazing to the situation of a notched tensile specimen. Finite element simulations are performed under 2D plane strain conditions. Figure 5b shows the computed plastic zone which displays the characteristic elongated shape observed in real ABS (Fig. 5a).

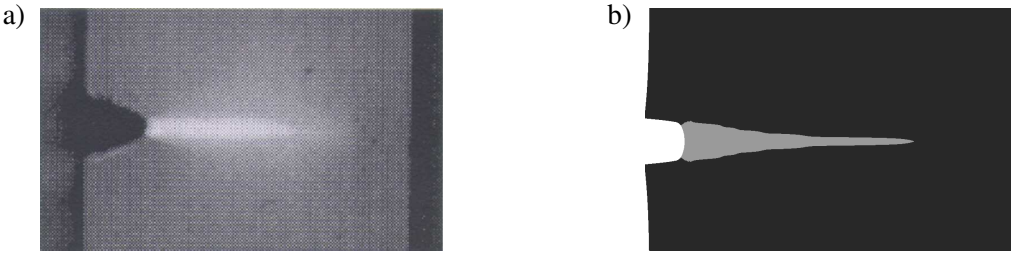

Figure 5: Plastic zone at notch in SENT specimen: a) experiment [9], b) simulation

Acknowledgment

Financial support of this work by the German Science Foundation (DFG) under grant no. SE 872/5-2 is gratefully acknowledged. We would also like to thank Prof. Arild H. Clausen for support with the experiments performed at SIMLab (NTNU Trondheim) and the DAAD for funding the visit to SIMLab.

References

[1] Bernal, C.R., Frontini, P.M., Sforza, M., Bibbo, M.A., *J. Appl. Pol. Sci.*, **1995**, 58, 1-10
[2] Bucknall, C.B., *Toughened Plastics*. Applied Science, London, 1977
[3] Gearing, B.P., Anand, L., *Int. J. Solids Structures* **2004**, 41, 3125-3150
[4] Ishikawa, M., *Polymer*, **1995**, 36, 2203-2210
[5] Pijnenburg, K.G.W., Seelig, Th., Van der Giessen, E., *Eur. J. Mech. A/Solids*, **2005**, 24, 740-756
[6] Ramaswamy, S., Lesser, A.J., *Polymer* **2002**, 43, 3743-3752
[7] Seelig, Th., Van der Giessen, E., *Comp. Mat. Sci.* **2009**, 45, 725-728
[8] Socrate, S., Boyce, M.C., Lazzeri, A., *Mech. Mater.*, **2001**, 33, 155-175
[9] Steenbrink, A.C., *Shaker* PhD thesis, TU Delft, **1998**
[10] Tijssens, M.G.A., Van der Giessen, E., Sluys, L.J., *Mech. Mater.* **2000**, 32, 19-35